

Suppression of the Shastry-Sutherland phase in $\text{Ce}_2\text{Pd}_2\text{Sn}$ at a field-induced critical point

J. G. Sereni,¹ M. Gómez Berisso,¹ G. Schmerber,² and J. P. Kappler²

¹División Bajas Temperaturas, Centro Atómico Bariloche, CNEA, 8400 S.C. Bariloche, Argentina

²IPCMS, UMR 7504, CNRS-ULP, 23 rue de Loess, BP 43, Strasbourg Cedex 2, France

(Received 5 February 2010; revised manuscript received 30 April 2010; published 24 May 2010)

The magnetic phase diagram of $\text{Ce}_2\text{Pd}_2\text{Sn}$ is investigated through the field dependence of thermal, transport, and magnetic properties at low temperature. The upper transition, $T_M=4.8$ K is slightly affected by magnetic field up to $B=1$ T whereas the lower one $T_C(B)$ rapidly increases from 2.1 K joining T_M in a critical point at $T_{cr}=(4.1 \pm 0.2)$ K for $B_{cr}=(0.11 \pm 0.01)$ T. At that point, the intermediate phase, previously described as an unstable Shastry-Sutherland lattice, is suppressed. A detailed analysis around the critical point reveals a structure in the maximum of the $\partial M / \partial B(B)$ derivative, which may be related to a step in magnetization predicted by theory for the mentioned lattice.

DOI: 10.1103/PhysRevB.81.184429

PACS number(s): 75.20.Hr, 71.27.+a, 75.30.Kz

I. INTRODUCTION

Complex or metastable phases are favored in the proximity of magnetic transitions since, within the Landau theory, the change in sign of the first term of the free energy $G(\psi)$ broadens its minimum as a function of the order parameter ψ as $T \rightarrow T_C$. In these critical conditions, the “roughness” of $G(\psi)$, occurring in real systems, may present relative minima which may become relevant in the formation of novel phases.¹ In recent years, an increasing number of magnetic systems exhibiting nontrivial types of order parameters have been reported. Those complex phases may correspond to magnetically frustrated systems such as “spin ice,”² Shastry-Sutherland (ShSu) lattice,^{3,4} or other exotic phases. Those phases can be tuned by nonthermal control parameters such as pressure (e.g., in pressure-induced superconductors⁵) or by magnetic field [e.g., in $\text{Sr}_3\text{Ru}_2\text{O}_7$ (Ref. 6)] and driven to a quantum critical point at $T=0$.⁷ Alternatively, some of those phases become unstable under moderate variation in the external parameters and are suppressed in a critical point at finite temperature.

The Shastry-Sutherland ShSu lattice can be described as a two-dimensional (2D) simple squared lattice, where nearest-neighbor (nn) and next-nearest-neighbor (nnn) couplings (J and J' , respectively) are antiferromagnetic (AF).³ In the case where nn magnetic atoms form dimers disposed in an orthogonal network, [e.g., $\text{SrCu}_2(\text{BO}_3)_2$ (Ref. 8)] the configuration is topologically equivalent to the 2D square lattice Heisenberg model⁴ which has an exact dimer ground state. Some peculiar features were observed in $\text{SrCu}_2(\text{BO}_3)_2$, such as quantized magnetization plateaux at fractional values (cf. 1/4 and 1/8) of the saturation moment and the crossing of magnetization isotherms as a function of applied field at certain temperatures.⁸

A stable ShSu phase in a rare-earth intermetallic compound was observed in $\text{Yb}_2\text{Pt}_2\text{Pb}$ single crystals,⁹ which undergoes a slight shift of part of Pt atoms that results in two types of Yb-Pt tetrahedral sublattices. Recently, the formation of that phase was also reported to form in $\text{Ce}_2\text{Pd}_2\text{Sn}$.¹⁰ That phase is observed within a limited range of temperature, between $T_M=4.9 > T > T_C=2.1$ K, having as the upper limit a correlated paramagnetic phase and a ferromagnetic (FM)

one as ground state (GS). This exotic phase builds up from FM dimers formed by Ce nn atoms, and shows the onset of magnetic correlations at $T \leq 20$ K. An AF exchange interaction between those dimers drives the formation of the ShSu phase, realized in this compound as a quasi-2D square lattice of effective spin $S_{eff}=1$ below $T_M=4.9$ K.¹⁰

This compound presents a unique crystalline Ce lattice where the mentioned exotic phase becomes unstable at T_C , undergoing a first order to a FM-GS. Neutron-diffraction experiments¹¹ revealed a modulated character of this phase, with the local moments pointing in the “c” crystallographic direction. The incommensurate propagation vector [qx] changes from 0.11 (at 4.2 K) to 0.077 (at 2.8 K) where it suddenly drops to [$qx=0$] once the long-range FM order parameter sets on.

Since the mentioned magnetic phase becomes unstable below 2.1 K, it only holds within a short range of temperature and the application of external field is expected to produce significant effects including its eventual suppression in a critical point. To our knowledge, there are no systematic investigations of magnetic phase diagrams for $\text{Ce}_2\text{T}_2\text{X}$ compounds (with $T=\text{Ni, Cu, Pd, Rh, and Pt}$ and $X=\text{Sn and In}$) performed yet. This is not a minor point since in the last years, a big effort was done searching for critical points at very low temperature and magnetic field may fine tune the critical conditions. Furthermore, the scarce examples for FM critical points places the $\text{Ce}_2\text{T}_2\text{Sn}$ family of compounds as good candidates for that current topic since it builds up from Ce atoms disposed in triangular prisms mimicking those of CeT (Ref. 12) FM compounds.

Preliminary studies on the effect of the magnetic field¹³ on $\text{Ce}_2\text{Pd}_2\text{Sn}$ showed that the upper transition is overcome by the lower one by applying moderate magnetic field. In order to investigate the characteristics of that critical region, we have performed a detailed investigation of the magnetic field effects on the low-temperature thermal, magnetic, and transport properties of this compound. Such a study allows to assemble a magnetic phase diagram including the critical point where the intermediate phase is suppressed.

II. EXPERIMENTAL DETAILS AND RESULTS

Details of sample preparation were described in a previous paper.¹⁰ Structural characterization confirms the single-

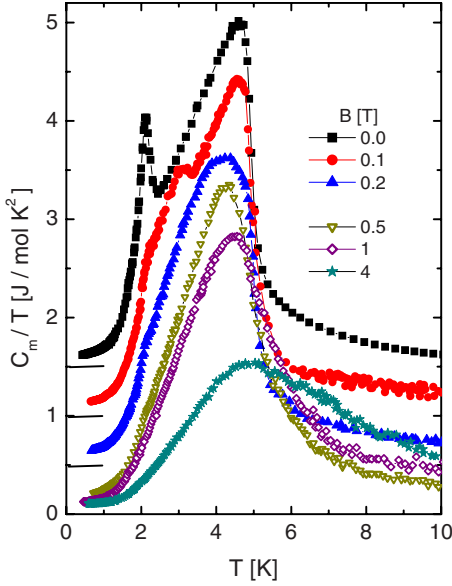


FIG. 1. (Color online) Effect of applied magnetic field up to 4 T on the specific heat after phonon subtraction. For clarity, curves at $B=0.2$, 0.1 , and 0 T are progressively shifted by 0.5 J/mol K 2 .

phase composition of the sample in a tetragonal Mo₂FeB₂-type structure with $a=7.765$ Å and $c=3.902$ Å lattice parameters. The actual composition of the sample was determined to be Ce_{2.005}Pd_{1.998}Sn_{0.997} after scanning electron microscopy/energy dispersive x-ray analysis. Specific heat was measured using the heat-pulse technique in a semiadiabatic He-3 calorimeter in the range between 0.5 and 20 K, at zero and applied magnetic field up to 4 T. dc-magnetization measurements were carried out using a standard superconducting quantum interference device magnetometer operating between 2 and 300 K, and as a function of field up to 5 T. Electrical resistivity was measured between 0.5 K and room temperature using a standard four-probe technique with an LR700 bridge.

The magnetic contribution C_m to the measured specific heat C_P was computed as in Ref. 10 subtracting the phonon contribution extracted from the isotropic compound La₂Pd₂Sn as $C_m=C_P-C_P(\text{La}_2\text{Pd}_2\text{Sn})$. As shown in Fig. 1, the magnetic field affects quite differently the specific-heat $C_m(T)$ anomalies of both transitions. While the temperature of the lowest ($T_C=2.1$ K) rapidly increases with field, the upper one defined as the maximum slope of ($T_M=4.9$ K) remains practically unaffected up to $B=0.2$ T. The well-defined first-order transition at $T_C(B=0)$ transforms into a broaden anomaly by the effect of applied field, which extends between $2 \leq T \leq 3$ K for $B=0.1$ T. Such a broadening is due to the polycrystalline nature of the sample since the crystals are randomly oriented between the easy and hard directions of magnetization. This random orientation yields to a continuous distribution of transitions according to the respective projections of the crystals respect to the magnetic field and, as it can be seen in Fig. 1, a small fraction of crystals oriented on their hard magnetization direction keep contributing at T_C up to $B=0.2$ T.

The fact that T_M is practically not affected up to $B=0.2$ T and, instead of deceasing, the maximum of C_m/T

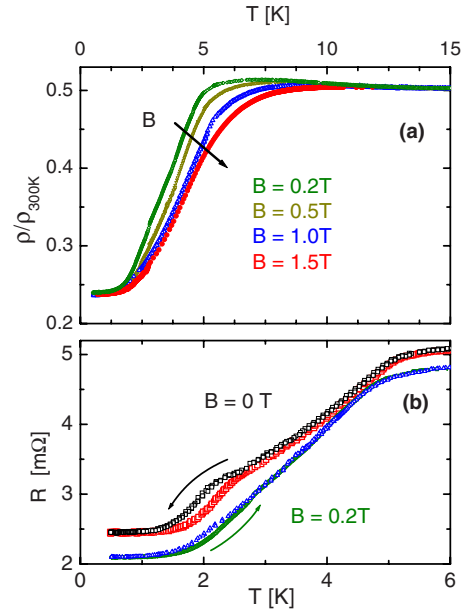


FIG. 2. (Color online) Effect of applied magnetic field on the electrical resistivity (a) for fields $B \geq 0.2$ T and $T < 3T_M$ and (b) comparison between zero and $B=0.2$ T showing the hysteresis of the lower (T_C) first-order transition.

starts to shift to higher temperatures at $B=4$ T are further evidences that the upper transition cannot be considered as AF in a canonical sense. However, such a weak variation in $C_m(T, B)$ indicates that the argument used in Ref. 10 to recognize the formation of Ce-Ce pairs remains valid at those fields.

Low-temperature resistivity measurements $\rho(T, B)$ are shown in Fig. 2, where the kink around 5 K indicates the upper transition T_M . The slight increase observed at $B=0$ of $\rho(T)$ approaching T_M from the paramagnetic phase was attributed to magnetic fluctuations related to a weak Kondo effect¹⁰ since the Kondo temperature of this compound was evaluated as $T_K \approx 3$ K.¹⁴ The application of magnetic field progressively quenches those fluctuations which practically disappear for $B=1$ T, with a concomitant broadening and shift to higher temperature of the upper transition for fields $B > 0.5$ T, see Fig. 2(a). Within the ordered phases (i.e., $T \leq 5$ K), the comparison between zero and $B=0.2$ T shows that $T_M(B)$ slightly decreases [see Fig. 2(b)] before to increase as depicted in Fig. 2(a).

Concerning the lower transition, a further kink in $\rho(T)$ signs the T_C temperature and the related hysteresis evidences its first-order character, see Fig. 2(b). A field of 0.2 T produces a strong reduction in the hysteresis and a moderate increase in T_C . There is a clear difference in the $\rho(T)$ curvature within the $2 < T < 5$ K range between zero and $B=0.2$ T. While at zero field, it shows a positive curvature, at $B=0.2$ T it looks practically linear. This difference, together with the vanishing hysteresis suggest a significant modification in the electronic scattering respect to zero field, which is probably related to a modification in the magnetic structure of the system in that range of temperature. As shown in Ref. 10, below T_C , the $R(T)$ dependence is very well described by a function proposed for anisotropic three-dimensional (3D) FM systems.¹⁵

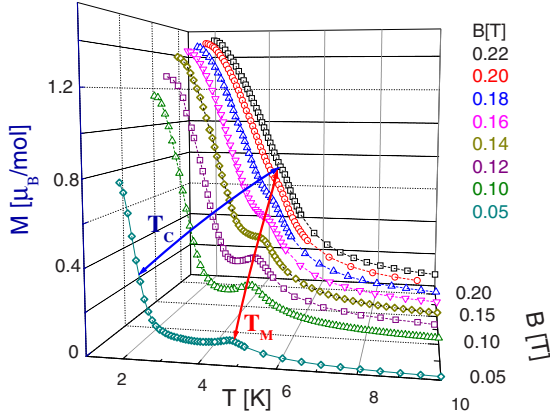


FIG. 3. (Color online) Temperature dependence of the magnetization for different applied fields, between 50 mT and 0.22 T. Solid curves the respective T_C and T_M field dependencies.

The $M(T)$ dependence was measured in different applied fields, starting from $B=0.05$ T. Between 0.1 and 0.22 T, the isodyna curves $M(T)|_B$ were measured with steps of 0.02 T as shown in Fig. 3. The presence of a cusp in $M(T)$ at T_M reveals that some types of AF interactions play a persistent role in the magnetic structure below that temperature and the $T_M(B)$ dependence is used to determine the field dependence of the upper phase boundary. At lower temperature, $M(T,B)$ results show how the FM phase overcomes the modulated one as it will be discussed in the phase diagram of Fig. 6.

Isothermal $M(B)$ measurements were performed within the $2 \leq T \leq 6$ K range of temperature up to $B=1$ T. In Fig. 4, we present the low-field magnetization curves (up to 0.3 T and 5 K), which shows the typical FM dependence at $T=2$ K, including a weak hysteresis (not shown for clarity) between increasing and decreasing field. Notice that our lower experimental limit of 2 K practically coincides with T_C . Above the transition (i.e., $T \geq 2.5$ K), $M(B)$ shows an S-shape dependence indicating that a rearrangement of the magnetic structure occurs. The broaden curvature of the $M(B)$ deviation from the linear dependence at low field was

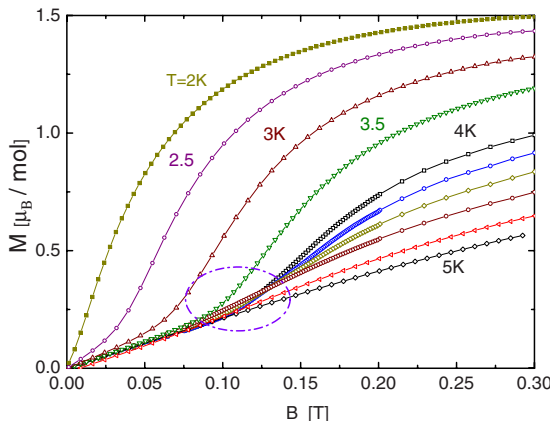


FIG. 4. (Color online) Isothermal field dependence of magnetization up to 0.3 T for the intermediate phase ($T_C < T < T_M$). Between 4 and 5 K, the measurements were carried every 0.1 K but represented every 0.2 K for clarity. The marked area centered at $B=0.12$ T is discussed in the text.

originally attributed to the random distribution of the magnetic directions in this polycrystalline and strongly anisotropic compound. However, a deeper analysis indicates that the $M(B)$ isotherms have not a monotonous variation in that region because they cross each other between 4 and 4.6 K around 0.12 T, see the remarked region in Fig. 4. This behavior suggests that the S shape (cf. the lack of metamagnetic discontinuity) can be also related to some intrinsic change in the order parameter and thus to the GS of this peculiar magnetic lattice. Furthermore, the comparison between $M(B)$ measurements on polycrystalline⁸ and single-crystalline¹⁶ samples of the model compound $\text{SrCu}_2(\text{BO}_3)_2$ show the same features. Interestingly, this $M(B,T)$ crossing occurs at a similar temperature than in $\text{Ce}_2\text{Pd}_2\text{Sn}$ (i.e., ≈ 4 K) despite the $M(T)$ maximum in $\text{SrCu}_2(\text{BO}_3)_2$ occurs at much higher temperature $T \approx 20$ K.

III. DISCUSSION

A simple thermodynamic analysis of the field effect on the thermal dependence of the specific heat allows to extract some trends concerning the magnetic behavior of the system. From Fig. 1, one sees that at low field ($B \leq 0.2$ T), $C_m(B)/T|_T$ slightly increases below T_M and consequently $S_m(B)|_T$ computed as $\int C_m(T)/TdT$. From Maxwell relations, such increase in $S_m(B)|_T$ corresponds to the observed increase in $M(T)$ as $T \rightarrow T_M$ (from below) since $\partial S_m/\partial B|_T = \partial M/\partial T|_H > 0$. On the contrary, at higher fields (i.e., $B \geq 0.5$ T), an induced FM behavior is reflected in a strong $\partial S_m/\partial B|_T$ decrease. This change in behavior reveals that the apparent AF character of the intermediate phase is overcome by a FM behavior around 0.2 T. Altogether, $S_m(T,B)$ dependence is slightly affected by magnetic fields up to 0.2 T but it progressively shifts to higher temperature for stronger fields. Nevertheless, $S_m(T)$ reaches the full expected value of $2R \ln 2$ at $T \approx 20$ K even for $B=1$ T.

Since in applied magnetic field, the specific-heat jump is progressively smeared by the mentioned random orientation of individual crystals and the maximum (negative) slope of $\partial M/\partial T|_B$ at $T=T_C$ is not properly defined, a more precise procedure to determine the phase boundary is required for a phase diagram construction. For such a purpose, we took as phase boundary the critical field B_C at which the maximum curvature of $M(B)$ occurs (see Fig. 4). Thus, we have analyzed the field dependence of the isothermal derivatives between 2 and 5 K. In Fig. 5(a), we show the second derivative $\partial^2 M/\partial B^2|_T$ between 2 and 4.5 K. There, one can see that B_C increases proportionally to the temperature up to about 4 K where an unexpected satellite anomaly appears at higher field.

In order to elucidate whether that second maximum is a systematic feature, we have performed detailed measurements of $M(B)$ between 3.8 and 4.7 K up to $B=0.3$ T and computed the corresponding derivatives as depicted in Fig. 5(b) in an expanded scale. One can see that between $4.1 \leq T \leq 4.4$ K, the satellite maximum appears around $B=0.15$ T and then vanishes for $T > 4.6$ K. This feature can be related to a modulation in $M(B)$, which in $\text{SrCu}_2(\text{BO}_3)_2$ (Ref. 8) corresponds to the formation of a plateau in the

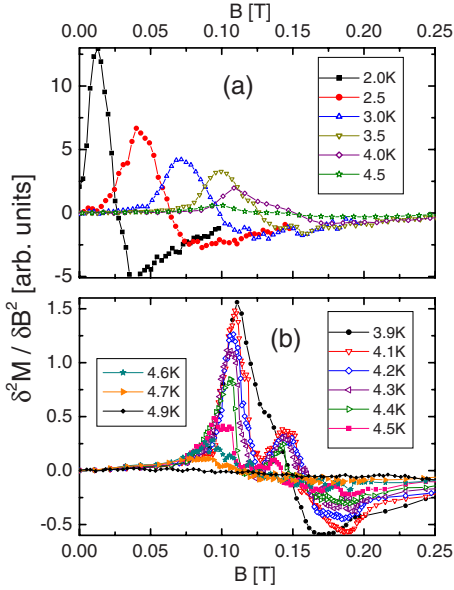


FIG. 5. (Color online) Second derivatives of $M(B)$ isotherms (a) between 2 and 4.5 K and (b) from 4 to 4.6 K showing a modulation in the $M(B)$ dependence between $4.1 \leq T \leq 4.4$ K (open symbols).

magnetization. Such a feature was predicted by the theory⁴ to occur at 1/4, 1/8, and 1/10 of the saturated moment M_S as a consequence of successive steps of commensuration in the magnetic ShSu lattice and identified as a “quantized magnetization.”⁸ In the case of $\text{Ce}_2\text{Pd}_2\text{Sn}$, only one modulation in $M(B)$ can be claimed to that respect and corresponds to the minimum of $\partial^2 M / \partial B^2|_T$ at $B \approx 0.13$ T. Interestingly, that field correspond to the crossing point of $M(B)|_{4 < T < 4.6}$ K and to a magnetization value of $0.35 \mu_B/\text{mol}$, which is close to 1/4 of the saturation moment $M_S = 1.53 \mu_B/\text{mol}$.

The resulting magnetic phase diagram is presented in Fig. 6. There, the field-driven phase boundary between the intermediate ShSu phase and the FM GS is drawn according to the maximum of $\partial^2 M / \partial B^2|_{max}$ in Fig. 5(a), which is in good agreement with C_m/T measurements, and the first maximum from Fig. 5(b). The alternative construction of the phase boundary following the temperature of the maximum slope of $\partial M / \partial T|_B$ (not shown) is not considered as a good determination of T_C because the FM contribution to $M(T)$ is superposed to the AF one below T_M . That mutual overlap increases as the system approaches the critical point as it can be seen in Fig. 3. The upper phase boundary, between the paramagnetic and the intermediate ShSu phase is properly defined by the cusp at $M(T_M)$. Since T_M is slightly affected by field in comparison to $T_C(B)$, both phase boundaries join at a critical point, at $T_{cr} = (4.1 \pm 0.2)$ K for $B_{cr} = (0.11 \pm 0.01)$ T.

From that phase diagram we recognize that, by cooling, the system: (i) develops a correlated paramagnetic region below about 15 K and $B < B_{cr}$, where dimers interaction (J) starts to develop, (ii) for higher fields, the induced Zeeman slitting becomes more important as it is shown in the modification of the tail of C_m/T in Fig. 1, and (iii) the lower phase boundary $T_C(B)$ increases proportionally to B . This behavior can be regarded as the competition between interdimer interaction J' and a FM interplanes interaction J_C between Ce

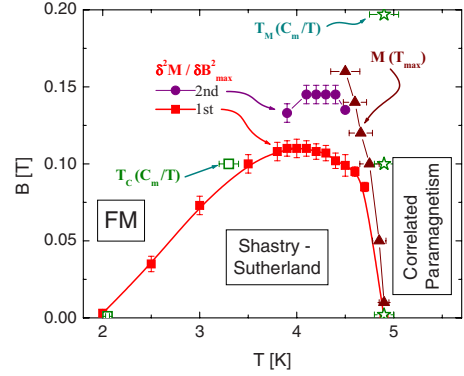


FIG. 6. (Color online) Field vs temperature phase diagram determined from (i) the cusp of $M(T, B)$ at $T_M(B)$ (full triangles) extracted from Fig. 3, (ii) $T_C(B)$ (full squares) the maximum curvature of $M(B)$ isotherms, i.e., $\partial^2 M / \partial B^2|_{max}$ shown in Figs. 5(a) and 5(b), and (iii) the second maximum of $\partial^2 M / \partial B^2|_{max}$ (full circles) indicating the region where a modulation of $M(B)$ occurs. Open symbols correspond to $C_m(T)/T$ data: (stars) $T_M(B)$ taken from the upper transition and (squares) T_C from the lower one. Error bars, vertical: B indetermination for field-dependent measurements, horizontal: T indetermination for thermal dependence.

layers. In fact, it was shown in Ref. 10 that below T_C , the electrical resistivity and specific heat are well described by respective functions for anisotropic 3D FM.^{15,17} Then, one concludes that the FM phase builds up from the local moments of Ce ions themselves once the interplane interaction “ J_c ” takes over transforming the 2D ShSu magnetic lattice into a normal 3D-FM.

As mentioned before, the magnetic structure of the intermediate phase has a modulated character¹¹ and its incommensurate propagation vector on the basal plane [qx] changes from 0.11 around T_M to 0.077 approaching T_C , where it drops to [$qx=0$] explaining the first-order character of the transition at $B=0$. The presence of magnetic field probably increases the length of the oscillations favoring the system dropping into the FM-GS at higher temperature and reducing the latent heat involved in the transition.

As proposed in Ref. 10 for $B=0$, Ce nearest neighbors form FM pairs with effective spin $S_{eff}=1$ which define a simple 2D square lattice lying parallel to the basal plane. A ShSu phase builds up from those dimers at $T=T_M$ which interact AF among them through the J' interaction. From the present results, we observe that dimers keep forming under moderate external field. However, the fact that the $C_m(T_C)$ jump and the height of the $\partial M / \partial B|_T$ maxima decrease as $T_C(B) \rightarrow T_M$ indicates that the degrees of freedom involved in the formation of the intermediate phase are progressively reduced by increasing magnetic field.

Above B_{cr} , the field at which the second maximum of Fig. 5(b) appears is also represented in Fig. 6 (full circles). As mentioned before, the structure observed in the $\partial^2 M / \partial B^2|_T$ as a function of field may correspond to one of the plateaus predicted in the $M(B)$ dependence by the theory and observed in $\text{SrCu}_2(\text{BO}_3)_2$, which in this case corresponds to $\approx 1/4$ of the saturated moment M_S . The weakness of this effect can be attributed to the metallic and polycrystalline character of the samples. At higher field ($B \geq 0.5$ T), the

induced Zeeman splitting starts to contribute to the specific-heat anomaly progressively shifting its maximum to higher temperature in coincidence with the broadening of the kink of $\rho(T)$ [see Fig. 2(a)].

IV. CONCLUSIONS

The field-dependent magnetic phase diagram was established for $\text{Ce}_2\text{Pd}_2\text{Sn}$. The application of magnetic field confirms that the transition at $T=T_M$ cannot be regarded as a canonical AF transition. On the contrary, the low-temperature FM phase is favored by field since the AF interaction among dimers in the intermediate phase is progressively suppressed.

The instability of the intermediate Shasry-Sutherland phase respect to the FM GS in this compound is confirmed by the low value of applied field $B_{cr} \approx 0.11$ T required for its suppression at $T_{cr}=4.1$ K. Around that critical region, a crossing of $M(B)$ isotherms is observed in a limited tempera-

ture range at $B \approx 0.13$ T, in coincidence with the appearance of a second maximum in the $\partial M^2 / \partial B^2(B)$ dependence. That anomalous behavior can be related to a weak modulation of $M(B)|_T$, reminiscent of the plateaux predicted by theory in that peculiar magnetic lattice.

Further investigations in oriented single-crystalline samples are required to confirm the origin of such anomalous feature. Other studies are in progress in this family of compounds with the aim to tune this critical point by doping Ce ligands (cf. Pd) or modifying the stoichiometry taking profit of the extended range of solubility of these compounds when Sn is substituted by In.¹⁸

ACKNOWLEDGMENTS

We acknowledge J. Luzuriaga and K. Ogando for their contribution to magnetic measurements. This work was partially supported by PICT-2007-812 (Foncyt) and Secyt-UNC project 6/C268. J.G.S. and M.G.B. are members of CONICET and Instituto Balseiro (UN Cuyo) of Argentina.

¹T. R. Kirkpatrick and D. Belitz, *Phys. Rev. B* **67**, 024419 (2003).

²R. Higashinaka, H. Fukazawa, K. Deguchi, and Y. Maeno, *J. Phys. Soc. Jpn.* **73**, 2845 (2004).

³B. S. Shastry and B. Sutherland, *Physica* **108B**, 1069 (1981).

⁴S. Miyahara and K. Ueda, *Phys. Rev. Lett.* **82**, 3701 (1999).

⁵A. P. Mackenzie and S. A. Grigera, *Science* **309**, 1330 (2005).

⁶A. G. Green, S. A. Grigera, R. A. Borzi, A. P. Mackenzie, R. S. Perry, and B. D. Simons, *Phys. Rev. Lett.* **95**, 086402 (2005).

⁷H. v. Löhneysen, A. Rosch, M. Vojta, and P. Wölfle, *Rev. Mod. Phys.* **79**, 1015 (2007).

⁸H. Kageyama, K. Yoshimura, R. Stern, N. V. Moshnikov, K. Onizuka, M. Kato, K. Kosuge, C. P. Slichter, T. Goto, and Y. Ueda, *Phys. Rev. Lett.* **82**, 3168 (1999).

⁹M. S. Kim, M. C. Bennett, and M. C. Aronson, *Phys. Rev. B* **77**, 144425 (2008).

¹⁰J. G. Sereni, M. Gómez-Berisso, A. Braghta, G. Schmerber, and J. P. Kappler, *Phys. Rev. B* **80**, 024428 (2009).

¹¹D. Laffargue, F. Fourgeot, F. Bouree, B. Chevalier, T. Roisnel, and J. Etourneau, *Solid State Commun.* **100**, 575 (1996).

¹²See, for example, J. G. Sereni, in *Handbook for Physics and Chemistry of Rare Earths*, edited by K. A. Gschneidner, Jr. and L. Eyring (Elsevier Science B.V., Amsterdam, 1991), Vol. 15, Chap. 98.

¹³M. Gómez Berisso, J. G. Sereni, A. Braghta, G. Schmerber, B. Chevalier, and J. P. Kappler, *Physica B* **404**, 2930 (2009).

¹⁴A. Braghta, G. Schmerber, A. Deroy, J. G. Sereni, and J. P. Kappler, *J. Magn. Magn. Mater.* **320**, 1141 (2008).

¹⁵E. Jobilong, J. S. Brooks, E. S. Choi, H. Lee, and Z. Fisk, *Phys. Rev. B* **72**, 104428 (2005).

¹⁶G. A. Jorge, R. Stern, M. Jaime, N. Harrison, J. Bonča, S. El Shawish, C. D. Batista, H. A. Dabkowska, and B. D. Gaulin, *Phys. Rev. B* **71**, 092403 (2005).

¹⁷S. N. de Medeiros, M. A. Continentino, M. T. D. Orlando, M. B. Fontes, E. M. Baggio-Saitovich, A. Rosch, and A. Eichler, *Physica B* **281-282**, 340 (2000); M. A. Continentino, S. N. de Medeiros, M. T. D. Orlando, M. B. Fontes, and E. M. Baggio-Saitovich, *Phys. Rev. B* **64**, 012404 (2001).

¹⁸M. Giovannini, H. Michor, E. Bauer, G. Hilscher, P. Rogl, T. Bonelli, F. Fauth, P. Fischer, T. Herrmannsdorfer, L. Keller, W. Sikora, A. Saccone, and R. Ferro, *Phys. Rev. B* **61**, 4044 (2000).